Statistical Physics

Wednesday, Sept. 2: 11:00 – 13:00

Session 3: MPI Lecture Hall

Contents

1

Effects of Shape on Diffusion

Rob Shaw[1] and Norman Packard[2]

[1] rob@haptek.com
[2] ProtoLife Inc., 6114 La Salle Ave, # 151, Oakland CA 94611
[2] European Center for Living Technology, S. Marco 2940 - 30124 Venezia, Italy
[2] Santa Fe Institute, 1399 Hyde Park Road, Santa Fe, New Mexico 87501

The motion of point particles undergoing random motions is of course well-understood; particle density can be considered a field, governed by the ordinary diffusion equation. The assumption that the infinitesimal particles do not interact leads to densities evolving according to a local and linear differential operator. But as soon as the motions of extended objects are considered, we may see unexpected effects due to nonlocal interactions, and deviations from standard Fickian diffusion. In fact, simple diffusive flow of shapes in confined spaces can be used in the construction of rectifiers, and other machines, on a microscopic scale. This is perhaps relevant in the highly crowded environment of the cytoplasm of living cells. Any sorting, or other operation, which can be accomplished in a simple gradient flow, without the expenditure of ATP, would be highly advantageous.

As a particular example, we examine rectification of ion flows in cellular membrane channels. While ion channels in today's living systems are highly sophisticated devices, we show that much of the functionality, including rectification, can be achieved simply with the geometrical constraints arising from extended objects in close proximity. No electrostatic binding, or additional cellular mechanisms are necessarily required.

The configuration space of a set of closely packed rigid objects can become convoluted, with many dead-end alleys. If the system is subjected to a shear, or gradient, it may naturally tend to settle in such a dead-end, and have to back up, or retrace its path, in order to proceed further. Thus metastable states, requiring a fluctuation to escape, can commonly arise, and a configuration can become locally locked. The requirement that the system backtrack to unlock distinguishes this process from ordinary jamming. There is no friction per se. We will present simple models of this process.

Even a Hamiltonian system of rigid extended objects in equilibrium can have complications. Ergodicity tells us that, in the long run, all configurations must be equally likely. But the space of configurations, subject to boundary conditions, may be constrained. Though the probability of being in any particular configuration is the same, the likelihood of getting in and out of a tight fit can be greatly reduced. For example, an object near a wall or a corner is more likely to remain for a time in a local area than an object in the bulk. Such extended residence times can affect reaction rates of molecules kept in proximity. We will suggest spatially dependent statistics to measure this effect.

We will present several examples, including simulations of hard disks in confined geometries, as well as dimers and other shapes moving on a lattice, and a few physical demonstrations.

References

1. N. Packard and R. Shaw, arxiv.org:cond-mat/0412626 (2004).
2. R. S. Shaw, N. Packard, M. Schröter and H. L. Swinney, *PNAS* **104**, p. 9580 (2007).

2

Nonequilibrium dynamics and finite size effects in stochastic condensation models

P. Chleboun and S. Grosskinsky

Centre for Complexity Science, Zeeman Building, University of Warwick, Coventry CV4 7AL, UK

Zero-range processes are driven diffusive systems where the number of particles per site is not restricted, allowing for particle accumulation. Under certain conditions on the parameters the zero-range process is known to exhibit a condensation transition [1]: When the particle density ρ exceeds a critical value ρ_c, the system phase separates into a homogeneous background with density ρ_c and all the excess mass concentrates on a single lattice site, forming the condensate. The stationary states of the system factorize, allowing for exact computations [1] and a rigorous mathematical analysis of this transition in terms of the equivalence of ensembles [2] under very general conditions.

Due to these results the zero-range process can be used as an effective model for phase separation and provides a very powerful cirterion in general driven diffusive systems [3]. There are many applications of these results in various areas (see [4] and references therein), and the zero-range process continues to be an important model for condensation phenomena, such as clustering in granular media (see [5] and references therein) and jam formation in traffic flow [6]. In applications, the thermodynamic limit is at best an idealization of large finite systems, so it is very important to understand finite size effects in these systems. A recent study on a perturbed zero-range process [7] revealed that these effects can be quite large and counterintuitive, even in the well established spatially homogeneous models, where they have been studied only in special cases so far [8].

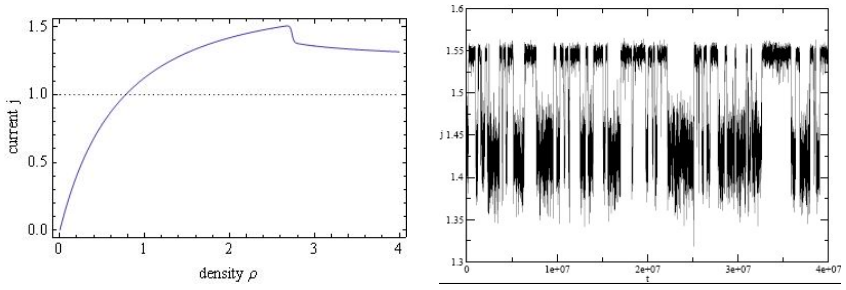

Fig. 2.1: Left: The current j as a function of the density ρ of a finite size zero-range process, showing a huge overshoot over the limiting maximal value $j = 1$. Right: Time series of the current j form a Monte Carlo simulation, showing switching between the condensed and the fluid phase.

We present a detailed analysis of finite size effects for the full class of models introduced in [1]. For some parameter values the effects are so strong,

that the finite system shows a metastable switching behaviour between the condensed and fluid phase, which is reminiscent of a first order phase transition (see Fig. 2.1). It is known that in the thermodynamic limit the transition is continuous, but they persist for very large system sizes and we argue that this can be particularly relevant to understand traffic flow patterns [9]. To gain a full understanding of this phenomenon we have to employ different techniques such as detailed saddle point computations, exact numerics to calculate free energies and stationary currents, truncation approximations and Monte Carlo simulations. Using a finer scaling to zoom into the behaviour at the critical point, the first order behaviour persists in the limit. We can define an effective free energy landscape with a double well structure and predict the switching times using the Arrhenius law. In this scaling limit the system shows many analogies with applications in granular media. The zero-range models applied in this area use generalized jump rates that depend also on the system size and exhibit metastibility and ergodicity breaking [10].

References

1. M.R. Evans, Phase transitions in one-dimensional nonequilibrium systems, Braz. J. Phys. **30**(1), 42—57 (2000)
2. S. Grosskinsky, G.M. Schütz, H. Spohn, Condensation in the zero range process: stationary and dynamical properties, J. Stat. Phys. **113**, 389 (2003)
3. Y. Kafri et al, Criterion for Phase Separation in One-Dimensional Driven Systems, Phys. Rev. Lett. **89**, 035702 (2002)
4. M.R Evans, T. Hanney, Nonequilibrium statistical mechanics of the zero-range process and related models, J. Phys. A **38**, R195 (2005)
5. D. van der Meer, K. van der Weele, P. Reimann, D. Lohse, Compartmentalized granular gases: flux model results, J. Stat. Mech. P07021 (2007)
6. J. Kaupuzs, R. Mahnke, R.J. Harris, Zero-range model of traffic flow, Phys. Rev. E **72**, 056125 (2005)
7. S. Grosskinsky, P. Chleboun, G.M. Schütz, Instability of condensation in the zero-range process with random interaction, Phys. Rev. E **78**, 030101(R) (2008)
8. S. Gupta, M. Barma, S.N. Majumdar, Finite-size effects on the dynamics of the zero-range process, Phys. Rev. E **76**, 060101 (2007)
9. R.E. Wilson, Mechanisms for spatio-temporal pattern formation in highway traffic models. Philos Transact A Math Phys Eng Sci. **366**, 2017 (2008)
10. S. Grosskinsky, G.M. Schütz, Discontinuous condensation transition and nonequivalence of ensembles in a zero-range process, J. Stat. Phys. **132**, 77 (2008)

3

Agent-Based Modelling for Molecular Self-Organization

S. Fortuna and A. Troisi

Chemistry Department and Centre for Scientific Computing, Warwick University, CV4 7AL, Coventry, United Kingdom

Self-organised molecular structures are ordered aggregates such as supramolecular liquid crystals [1], cell membranes, virus capsids [2], and synthetic supramolecular materials [3], held together by intermolecular forces. Although considerable progress has been made in the prediction of self-assembly structures, it is still generally not possible to predict the most stable structure formed by an aggregate of identical molecules [4]. Standard simulation methods as Molecular Dynamics (MD) or Monte Carlo (MC) are unable to correctly predict the most stable aggregates because the self-assembly process spans multiple time and length scales giving rise to a complicated free energy surface with many local minima [5], which act as kinetic traps for both types of simulation.

An alternative approach to the problem can be found considering that most self-assembling systems of interest are composed by a collection of identical particles, which are effectively searching for the same free energy minimum. Exploiting this symmetry of the system one can devise an algorithm that uses all identical particles to perform a parallel search of the global minimum. This idea, first proposed by Ratner et al. and initially implemented for lattice systems [6], is explored in this work where we propose and test a new Agent Based (AB) algorithm [7] for finding potential energy minima for off-lattice systems (of identical particles). AB algorithms have been developed and used to study complex systems in research areas very far from chemistry (e.g. economics [9], social sciences [10]).

Our system is composed by rigid particles in a fixed volume with periodic boundary condition (PBC). At the beginning of the simulation each agent coincides with a particle and, as the simulation proceeds, the agent evolves to represent stable portions of the system. The actions that an agent can perform are *move*, *merge*, *split* with the addition of the *disaggregate* action (not present in the lattice version of this algorithm [6]). The decision on which action to perform is based on a set of conditions which depend on the configurational energy of the system and on its past memory. The algorithm rules are described graphically in Fig. 3.1.

The rules are updated as the simulation proceeds, therefore the evolution of the system toward the most stable minimum is driven by a combination of adaptation (new configurations require new types of move) and learning (past successful choices should be repeated). Using this set of rules, the algorithm clusters the system "on the fly" in order to reduce the number of steps necessary to reach its lowest energy state.

The presented algorithm is designed to make it usable in conjunction with standard molecular mechanics computational packages and we have recently

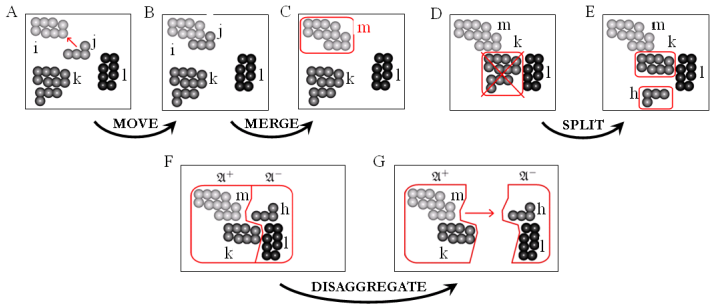

Fig. 3.1: Illustration of the basic actions that can be undertaken by the agents (set of particle). The agent j can perform a simple *move* in space (from A to B). The agents i and j can *merge* into a new agent m if their interaction energy is favourable (from B to C) and evolve in space as a unique body. If the energy of an agent k is too low compared with that of other agents in the simulation, it *splits* emitting a new agent h (from D to E). If a set of agents m, k, l, h form an aggregate (kinetic trap) they *disaggregate* (from F to G).

completed the implementation of an interface between this algorithm and the freely available Tinker molecular modelling package [8].

References

1. T. Kato, N. Mizoshita, and K. Kishimoto, Angew. Chem. Int. Ed. 45 (2006) 38.
2. J. A. A. W. Elemans, A. E. Rowan, and R. J. M. Nolte, J. Mater. Chem. 13 (2003) 2661.
3. J. M. Lehn, Chem. Soc. Rev. 36 (2007) 151.
4. S. M. Woodley and R. Catlow, Nat. Mater. 7 (2008) 937.
5. D. J. Wales and T. V. Bogdan, J. Phys. Chem. B 110 (2006) 20765.
6. A. Troisi, V. Wong, and M. A. Ratner, Proc. Natl. Acad. Sci. USA 102 (2005) 255.
7. M. Wooldridge, An Introduction to MultiAgent Systems, Chichester, 2002.
8. J. W. Ponder and F. M. Richards, J. Comput. Chem. 8 (1987) 1016.
9. J. Feigenbaum, Rep. Prog. Phys. 66 (2003) 1611.
10. C. Cioffi-Revilla, Comput. Math. Organ. Theory 15 (2009) 26.

4

Wet granular rafts: agglomeration in two dimensions under shear

Kai Huang[1,2], Martin Brinkmann[1], and Stephan Herminghaus[1]

[1] Max Planck Institute for Dynamics and Self-Organization, Bunsenstr.10, 37073 Göttingen, Germany
[2] Experimentalphysik V, Universität Bayreuth, D-95440 Bayreuth, Germany

We study clustering of hydrophobic sub-millimeter glass spheres trapped at an air-liquid interface and wetted by an oil phase under shear flow. The wetting liquid gives rise to a hysteretic and short ranged capillary force between adjacent particles due to the formation of liquid bridges(see Fig. 4.1). Clustering of particles is captured by a high speed camera and motions of individual particles are determined by an image processing procedure. We study the cluster size distribution at various amount of wetting liquid and shear rate ($\dot{\gamma}$). Fractal dimensions of clusters are found to be 1.63, fairly independent of $\dot{\gamma}$. The above experimental results agree well with our molecular dynamical (MD) simulations. A model based on the balance between capillary force and viscous drag force gives a relation ($N \propto \dot{\gamma}^{-0.8}$), between the shear rate $\dot{\gamma}$ for a clusters of size N to break. This is found to be in fair agreement with the experimental results.

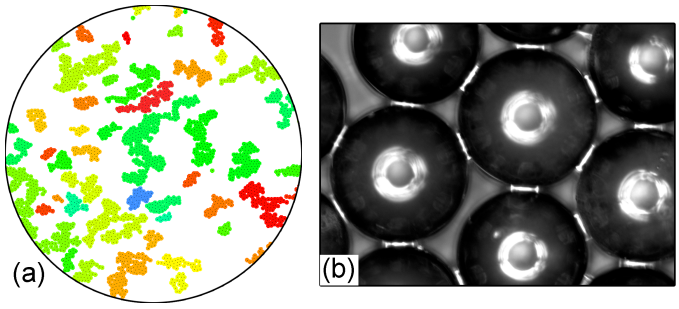

Fig. 4.1: a) Aggregates formed by wet particles trapped at air-liquid interface after image processing. Different clusters are coded with different colors and black dots correspond to the locations of particles found by the image processing procedure. (b) Close view of wet particles under microscope.

5

Periodic orbits and dynamics of sliding friction

A.S. de Wijn, C. Fusco, and A. Fasolino

Institute for Molecules, Radboud University Nijmegen, Heyendaalseweg 135, 6525 AJ Nijmegen, the Netherlands

The phenomenon of friction is one of the oldest problems in physics, and certainly one of the most important for practical applications. Nevertheless, so far remarkably little is understood about the fundamental microscopic processes responsible for friction and wear. As a result of increased control in surface preparation and the development of local probes like the atomic force microscope, recent years have witnessed a surge of interest in understanding the microscopic origin of friction [1].

Most models of sliding friction at the atomic scale are constructed by considering a mobile set of atoms representing a tip or an adsorbed atomic layer interacting with a rigid periodic substrate. The interaction between the mobile object and the substrate are usually nonlinear, and in order to make contact with experiments the motion is often driven.

For an extended object consisting of many atoms the effects of commensurability with the substrate (whether or not the atoms in the tip line up with the minima in the surface potential) become crucial. For an infinitely extended incommensurate contact the static friction has been shown to vanish [2]. Frictionless sliding of incommensurate contacts has also been predicted at finite and large velocities [3] and this effect has been named superlubricity. Extremely low friction has indeed been observed experimentally in several systems, for example W on Si [4] and graphite on graphite [5]. However, there is evidence that the incommensurate superlubric state is destroyed by rotation of the sliding flake [6], leading to a locking in a commensurate state with high friction and slip-stick behaviour.

In this work, we study the driven dynamics of a finite rigid graphite flake on a graphite surface. This interaction is modelled with a realistic static potential. By changing the orientation of the flake onto the hexagonal substrate the contact is either commensurate or incommensurate. For a commensurate contact, we always find a stick-slip behaviour with high friction. Conversely, for an incommensurate contact we find two types of qualitatively different behaviour. After an initial short period, the flake either rotates and locks into a commensurate orientation or it remains incommensurate and slides with extremely low friction. This behaviour is critically dependent on the initial conditions, as expected for a strongly nonlinear problem with 5 degrees of freedom.

We construct a simple 4-dimensional dynamical system which captures the essential properties of the system, and for which the stability analysis can be done analytically. The model system contains invariant manifolds which correspond to the commensurate and incommensurate states. Their stability depends on the parameters of the system, which are related to the substrate

potential. We show that for a realistic potential both the commensurate and incommensurate states may be stable.

References

1. For a review see e.g. A. Fasolino in Handbook of Theoretical and Computation Nanotechnology (ed. M. Rieth and W. Schommers) volume 5, pages 379-436, American Scientific Publishers (2006).
2. M. Peyrard and S. Aubry, J. Phys. C **16**, 1593 (1983).
3. K. Shinjo and M. Hirano, Surf. Sci. **283**, 473 (1993).
4. M. Hirano, K. Shinjo, R. Kaneko and Y. Murata, Phys. Rev. Lett. **78**, 1448 (1997).
5. M. Dienwiebel, G.J. Verhoeve, N. Pradeep, J.W.M. Frenken, J.A. Heimberg, and H.W. Zandbergen, Phys. Rev. Lett. **92**, 126101 (2006).
6. A.E. Filippov, M. Dienwiebel, J.W.M. Frenken, J. Klafter and M. Urbakh, Phys. Rev. Lett. **100**, 046102 (2008).

6

Driving forces and crack patterns in thin colloidal films

L. Goehring[1], A. F. Routh[1], and W. J. Clegg[2]

[1] BP Institute for Multiphase Flow, University of Cambridge, Madingley Rise, Madingley Road Cambridge, UK, CB3 0EZ
[2] Department of Materials Science and Metallurgy, University of Cambridge, Pembroke Street, Cambridge, CB2 3QZ

Paints and other thin films are so ubiquitous in our everyday lives, that 'watching paint dry' is literally synonymous with utter tedium. Diverse materials, such as latex paints, ceramics, artificial opals, and photonic crystals, are prepared as stable colloidal mixtures of some liquid dispersant, and solid particles a few tens, to a few hundreds of nanometers in diameter. Yet, despite being of immediate importance to both cutting edge scientific research, and established industries, the manner in which these materials solidify, and, as is often the case, crack, is still poorly understood.

We observed the drying of dispersions of polystyrene in water. A range of particle sizes, with diameters from 100-400 nm, were synthesized, and used to cast liquid films onto glass slides. Films were dried either by blowing nitrogen gas across them, or by leaving them in still air.

As water evaporates, the films dry first at their edges, leaving a slowly shrinking liquid area, as shown in Fig. 6.1(a). The particles are forced together by the removal of water, and reach a density where they coalesce into a solid. This rigid part of the film is dry to the touch, but the pore spaces between particles are still saturated with water. As such, evaporation continues to remove liquid from its upper surface. To replenish this loss, water flows from the liquid into the saturated region. This porous-media flow is equivalent, through Darcy's law, to a horizontal pressure gradient within the saturated film. When the film is flat, this leads to the growth of an array of parallel cracks, as shown in 6.1(a). When the film is slowly thickening, we present evidence of a dynamical instability, whereby every second crack slows down, and develops oscillatory behavior, as shown in 6.1(c). At some point, the capillary pressure exceeds that required to empty the inter-particle pores, and the film drains. In a surprisingly simple way, we will show that the capillary forces within the film can provide a driving force for the propagation of fractures, describe the deformation caused by the cracks, the process of delamination, and the scaling behavior of the crack pattern. There is a pressure difference across any liquid-air interface. Once a crack appears, the capillary forces on the crack surface puts surrounding particle network into compression. As the crack grows, energy is generated by the action of the surface pressure over the volume that the crack opens, which can balance both the energy used to deform the network, and the energy required to advance the crack. Furthermore, if the film is bound to a substrate, the opening of the crack will pull on the substrate, which can force the film to delaminate, and peel up.

All these effects were clearly seen in our drying latex films. Fluid flow through the saturated film was tracked by introducing aqueous dyes, and sur-

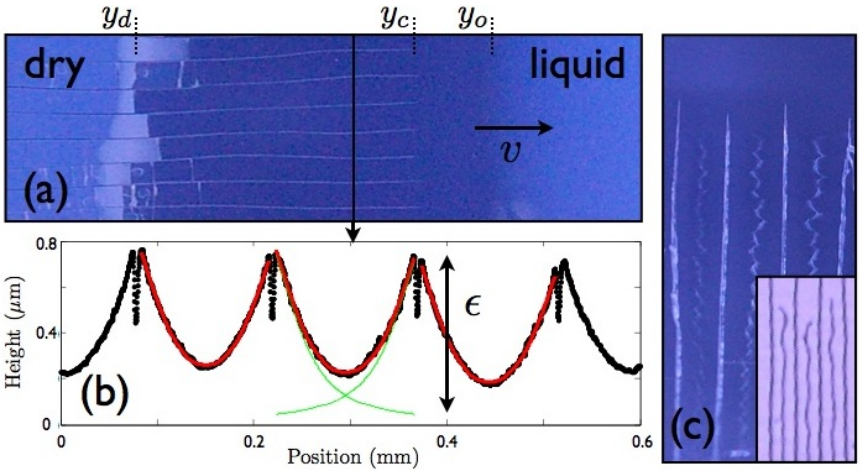

Fig. 6.1: Interesting and insightful crack patterns can form in a colloidal film (a) As a film dries, it changes from a liquid to a solid (y_0), cracks (y_c), and eventually fully dewets (y_d). In a directionally dried film, these fronts all advance with a speed v in the drying direction. (b) As the cracks open, they deform the surface of the film (black line). This strain is well fit by a model (red) of the sum of the strains (green) caused by compressive forces acting on the crack faces. The vertical strain, ϵ, increases in direct proportion to the capillary pressures caused by fluid flow. (c) When the experiment is inclined, such that the film is slowly thickening, the crack front can undergo a period doubling instability, followed by the development of oscillations in the cracks which lag behind.

face deformation was monitored, as the film dried, by scanning profilometry. As shown in Fig. 6.1(b), the shape of the deformed film surface was accurately captured by considering the response of a thin elastic body, bound to a rigid substrate, and subjected to compressive pressures on both the upper surface, and the crack faces. The magnitude of the strain increased in proportion to the capillary pressure, inferred from fluid flow measurements, and was greater in films with smaller particles.

7

Analytical study of shear-banding in a piecewise linear model

J.L.A. Dubbeldam[1] and P.D. Olmsted[2]

[1] Delft Institute of Applied Matematics, Delft University of Technology, Mekelweg 4, 2628 CD Delft, The Netherlands
[2] Polymer IRC and School of Physics and Astronomy, University of Leeds, United Kingdom

In shear banding the material splits into different spatial regions, or bands, that flow at different shear rates $\dot{\gamma}$. This phenomenon has been observed in granular media [1] and in viscoelastic living polymer systems such as wormlike micelle solutions [2]. Theoretically, shear banding is fairly well understood at the level of a stable one dimensional (1D) banding profile [3–5], which connects two shear rates that are stable at a given selected total shear stress Σ. Wormlike micelles, polymer melts, and liquid crystals naturally give rise to such bistable constitutive relations [6, 7]. However, the stability of bands in two or three dimensions (i.e. with respect to capillary-like fluctuations of the interface) is not well understood, despite a frequent interpretation in terms of a simple stable flat interface between coexisting states. It has been experimentally observed that the interface between the two phases is not necessarily flat, but can exhibit strong undulations and erratic fluctuations [8]. Theoretical calculations have shown that in shear banding flows, chaotic motion of shear bands can occur [9, 10].

A recent numerical calculation in two dimensions [11] demonstrated that, for the Johnson-Segalman (JS) model the interface between the low and high shear rate phases is *linearly unstable* to undulations. In this case the unstable mode involved normal stresses; however, it is still not known whether normal stresses are *carried by* an instability inherent in the two-dimensional (2D) nature of the fluctuation, or whether normal stresses *trigger* the instability. Hence, we consider a simple general toy model without normal stresses. We show that for a wide class of multivalued flow curves, a linear instability can never occur. Our findings imply that the coupling between convective terms and perturbations in shear stress cannot lead to a linear instability, which suggests that an instability requires other degrees of freedom, such as normal stresses.

We start from a model for the time evolution of the polymer stress σ_p

$$(\partial_t + \mathbf{v}\cdot\nabla)\,\sigma_p = \widehat{\Sigma}_0(\hat{\dot{\gamma}}) + D\nabla^2\sigma_p, \tag{7.1}$$

where $\widehat{\Sigma}_0(\hat{\dot{\gamma}})$ is a piecewise linear function of the shear rate $\hat{\dot{\gamma}}$; see Fig. 7.1. The diffusion constant D is typically small. In the creeping flow approximation the total shear stress Σ is

$$\Sigma = \sigma_p(y) + \eta\dot{\gamma}(y), \tag{7.2}$$

The stationary states can be found graphically by assuming a smooth solution to Eqs. (7.1) and (7.2) and correspond to intersection points of two families of curves as shown in Fig. 7.1 Solution A has two bands, B four bands etc.

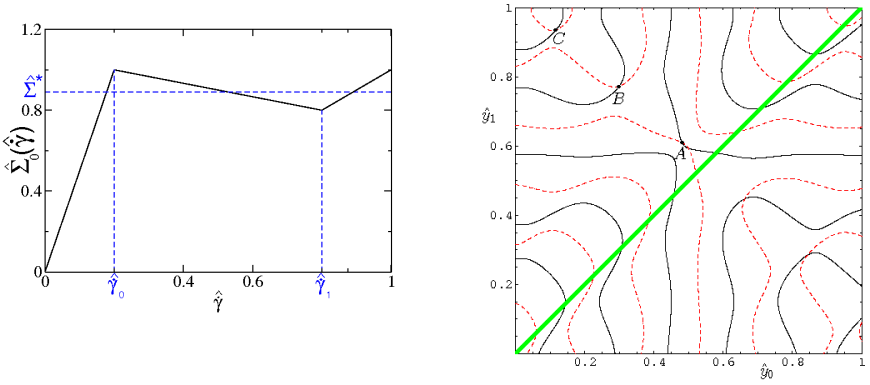

Fig. 7.1: The selected stress $\hat{\Sigma}^*$ and the piecewise linear function $\hat{\Sigma}_0(\hat{\dot{\gamma}})$ as a function of shear rate (left) and the stationary states appearing as intersection points of a family of curves (right).

Using Fourier techniques we show that solution A is neutrally stable, whereas all other solutions are linearly unstable. This demonstrates that to explain the linear instability of the JS model, as predicted by Fielding, normal stresses are imperative.

References

1. I. Cohen, B. Davidovitch, A. Schofield, M. Brenner, and D. Weitz, Physical Review Letters **97**, 215502 (2006).
2. V. Schmitt, F. Lequeux, A. Pousse, and D. Roux, Langmuir **10**, 955 (1994).
3. O. Radulescu and P. D. Olmsted, Rheol. Acta **38**, 606 (1999).
4. N. A. Spenley, X. F. Yuan, and M. E. Cates, J. Phys. II (France) **6**, 551 (1996).
5. C. Y. D. Lu, P. D. Olmsted, and R. C. Ball, Phys. Rev. Lett. **84**, 642 (2000).
6. T. Shimada, M. Doi, and K. Okano, J. Phys. Soc. of Japan **57**, 2432 (1988).
7. M. E. Cates, J. Phys. Cond. Matt. **8**, 9167 (1996).
8. M. R. Lopez-Gonzalez, W. M. Holmes, P. T. Callaghan, and P. J. Photinos, Phys. Rev. Lett. **93**, 268302 (2004).
9. M. E. Cates, D. A. Head, and A. Ajdari, Phys. Rev. E **66**, 025202 (2002).
10. S. M. Fielding and P. D. Olmsted, Phys. Rev. Lett. **92**, 084502 (2004).
11. S. M. Fielding, Phys. Rev. Lett. **95**, 134501 (2005).

8

Oscillation dynamics of soap bubbles

U. Kornek[1], K. Harth[1,2], R. Stannarius[1], A. Hahn[2], and L. Tobiska[2]

[1] Otto von Guericke University Magdeburg, Institute of Experimental Physics
[2] Otto von Guericke University Magdeburg, Institute of Analysis and Numerics

Oscillations of fluid volumes embedded in a fluid environment have been extensively studied since the 19^{th} century. These systems include, for example, liquid droplets in air, oil droplets in water, gas bubbles in liquids, vesicles and many others. Sizes range from micrometers to several centimeters and above.

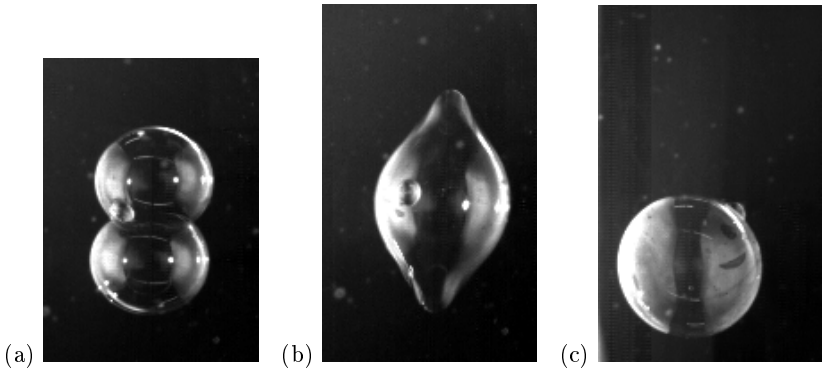

Fig. 8.1: Side view of an oscillating soap bubble, the first image (a) is taken immediately after coalescense, the time delays are 6 ms between images (a) and (b), and 276 ms between (b) and (c).

We investigate oscillations of soap bubbles consisting of very thin soap films that enclose an air volume and that are embedded in a gas. Similar structures can be conceived of smectic liquid crystals. The bubbles have radii of 1 cm and more. The gases inside and outside the bubbles contribute to the oscillations. This distinguishes our systems from liquid droplets in gas as well as from gas bubbles in liquids and leads to qualitatively different oscillation spectra. The membranes are so thin that their inertia can be neglected with respect to that of the gas volume. Although the inner gas volume is in principle compressible and not necessarily conserved, we find that we can assume volume conservation in good approximation. In that respect, the soap bubbles behave much similar to vesicles.

The driving forces for oscillations of thin membranes can be surface tension and bending stiffness. In our systems, we find that the latter can be neglected. Surface tension of the soap films plays the dominating role.

The initial states of deformed bubbles are prepared by two different methods. In both cases we bring two spherical bubbles in contact with each other and in most cases, the situation shown in Figure 8.1(a) of the coalescense of the

two bubbles is found. The shapes of such deformed bubbles are axisymmetric and remain so while the bubbles oscillate and relax towards the energetically favoured spherical final state. During the experiment the bubbles float on a layer of butane in a glass container. We observe them with a high-speed camera at frame rates between 1000 to 2000 frames per second. We record both top view and side view of the oscillating bubbles simultaneously, using a mirror at an angle of 45° above the bubble. The edges are detected and the edge shapes in each image are expanded in cylinder symmetric spherical harmonics. Those are considered as the eigenmodes of oscillations of the linearised system [1]. The time dependent amplitudes of these modes are exploited to analyse the frequencies, and damping constants, as well as anharmonic behavior of the modes.

Already in 1879, a model for an equivalent system was derived by Sir Horace Lamb under the assumptions of irrotional flow, incompressibility of the fluid and only small displacements of the surface from equilibrium. Although Lamb's model considers only small oscillations and thus neglects coupling of the modes, we find experimentally that oscillation frequencies of the second and higher modes are both qualitatively and quantitatively in good agreement with the predictions. In addition, the 0^{th} and 1^{st} modes in the experiment couple to higher modes owing to volume conservation and nonlinear effects.

In order to test Lamb's assumptions on the flow field and the validity of the linearized model, we employ a numerical programme that solves the Navier-Stokes equations by means of a finite elements algorithm with moving boundaries. This program allows the computation of bubble oscillations for arbitrary initial conditions and in particular for large deviations from the equilibrium shape. The coupling of the linear modes becomes evident. With the computational data, we can visualise the internal flow and pressure fields. In addition, the damping rates for the individual modes, which are not considered in Lamb's analytical treatment, can be computed and related to scaling parameters of the flow. We compare the results of the numerical calculations with our experimental data.

References

1. Sir H. Lamb, *Hydrodynamics*, Cambridge University Press (1932), p. 473 *ff*.

9

Extreme coherent events in discrete nonlinear lattices

G. P. Tsironis

Department of Physics, University of Crete, and Institute of Electronic Structure and Laser, Foundation for Research and Technology – Hellas, P. O. Box 2208, 71003 Heraklion, Greece first address

There are various reports by sailors regarding the appearance of extremely large amplitude sea waves referred to as rogue or freak waves. These waves appear very suddenly in relatively calm seas, reach amplitudes of over $20m$ and may destroy or sink small as well as large vessels [1]. Theoretical analysis of ocean freak waves has been linked to nonlinearities in the waver wave equations, studied though the nonlinear Schrödinger (NLS) equation and shown that the probability of their appearance is not insignificant [2]. In addition to sea waves there have been recent experimental observations of optical rogue waves in microstructured optical fibres; a generalized NLS equation was used to model the generation of optical rogue waves [3]. We present a numerical investigation on the role of integrability in the formation of discrete rogue waves (DRW) and the resulting extreme event statistics. We use the Salerno model [4] that through a unique parameter interpolates between a fully integrable discrete lattice, viz. the AL lattice [5] , and the nonintegrable DNLS equation [6, 7]. We address the probability of occurrence of a DRW as a function of the degree of integrability of the lattice and thus link the role of the latter in the production of extreme lattice events [8].

The Salerno model (SM) is given through the following set of equations

$$i\frac{d\psi_n}{dt} = -(1+\mu|\psi_n|^2)(\psi_{n+1}+\psi_{n-1}) - \gamma|\psi_n|^2\psi_n \tag{9.1}$$

where μ and γ are two nonlinearity parameters. When $\mu = 0$ the model becomes the DNLS equation while for $\gamma = 0$ it reduces to AL. We may use the parameter $\Gamma = \gamma/\mu$ to study the various regimens of the equation; we use a uniform initial condition with some quenched noise.

The statistics of the wave heights is probed through the time-averaged height distributions P_h. A DRW is defined as a wave that has a height greater than $h_{th} = 2.2h_s$, with h_s the significant wave height, i.e. the average height of the one-third higher wave. The probability of occurrence of extreme DRW events is then $P_{ee} = P_h(h > h_{th})$; we estimate P_{ee} as a function of the parameter Γ. We find that the probability for the occurrence of a DRW has a certain value in the AL case, peaks for small values of Γ and decays precipitously when $\Gamma >> 1$. This behavior of P_{ee} is compatible with the integrable AL modes interacting coherently in the weakly non-integrable regime leading to DB fusion and DRW generation. When nonintegrability becomes stronger, the scattering of the AL modes is more chaotic leading to a suppression of DRW formation. The probability of occurrence of extreme events P_{ee} in the SM results from the competition between the self-focusing and the energy transport mechanisms which are implicitly correlated with the degree of integrability of the model [9].

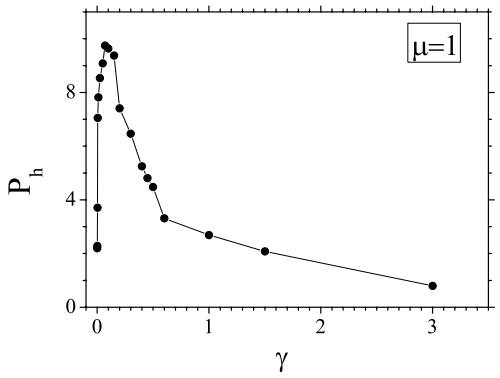

Fig. 9.1: Probability $P_{ee} = P_h(h \geq h_{th})$ for the occurrence of extreme events as a function of the integrability parameter Γ. All data present averaged results of five numerical measurements differing in the initial conditions.

References

1. P. Müller, C. Garrett, and A. Osborne, Oceanography **18**, 66 (2005).
2. M. Onorato, A. R. Osborne, M. Serio, and S. Bertone, Phys. Rev. Lett. **86**, 5831 (2001).
3. D. R. Solli, C. Ropers, P. Koonath, and B. Jalali, Nature **450**, 1054 (2007); J. M. Dudley, G. Genty, and B. J. Eggleton, Opt. Express **16**, 3644 (2008).
4. M. Salerno, Phys. Rev. A **46**, 6856 (1992).
5. M. J. Ablowitz and J. F. Ladik, J. Math. Phys. **17**, 1011 (1976).
6. C. H. Eilbeck, Lomdahl, Scott, Physica D **16**, 318 (1985).
7. M. Molina and G. P. Tsironis, Physica D, **65**, 267 (1993).
8. C. Nicolis, V. Balakrishnan, and G. Nicolis, Phys. Rev. Lett. **97**, 210602 (2006).
9. A. Maluckov, Lj. Hadžievski, N. Lazarides, G.P. Tsironis, Phys. Rev. E **79**, 025601 (2009).